International Journal of Nanomedicine

Dovepress
open access to scientific and medical research

Open Access Full Text Article

ORIGINAL RESEARCH

Effects of silver nanoparticles in combination with antibiotics on the resistant bacteria *Acinetobacter baumannii*

This article was published in the following Dove Press journal:
International Journal of Nanomedicine
12 August 2016
Number of times this article has been viewed

Guoqing Wan[1,2]
Lingao Ruan[2,3]
Yu Yin[2,3]
Tian Yang[2,3]
Mei Ge[2]
Xiaodong Cheng[1,4]

[1]School of Life Science and Technology, China Pharmaceutical University, Nanjing, [2]Shanghai Laiyi Center for Biopharmaceutical R&D, [3]School of Pharmacy, Shanghai Jiao Tong University, Shanghai, People's Republic of China; [4]Department of Integrative Biology & Pharmacology, The University of Texas Health Science Center, Houston, TX, USA

Abstract: *Acinetobacter baumannii* resistance to carbapenem antibiotics is a serious clinical challenge. As a newly developed technology, silver nanoparticles (AgNPs) show some excellent characteristics compared to older treatments, and are a candidate for combating *A. baumannii* infection. However, its mechanism of action remains unclear. In this study, we combined AgNPs with antibiotics to treat carbapenem-resistant *A. baumannii* (aba1604). Our results showed that single AgNPs completely inhibited *A. baumannii* growth at 2.5 μg/mL. AgNP treatment also showed synergistic effects with the antibiotics polymixin B and rifampicin, and an additive effect with tigecyline. In vivo, we found that AgNPs–antibiotic combinations led to better survival ratios in *A. baumannii*-infected mouse peritonitis models than that by single drug treatment. Finally, we employed different antisense RNA-targeted *Escherichia coli* strains to elucidate the synergistic mechanism involved in bacterial responses to AgNPs and antibiotics.

Keywords: *Acinetobacter baumannii*, AgNPs, synergistic, antibiotic combination, antisense RNA

Introduction

Drug-resistant *Acinetobacter baumannii* is an infectious pathogen that currently presents serious clinical challenges. *A. baumannii* is particularly associated with hospital-acquired infections such as pneumonia, bloodstream, abdominal, central nervous system, urinary tract, and skin and soft tissue infections.[1] *A. baumannii* can develop resistance against antibiotics through several mechanisms;[2] in particular, this bacterium is often resistant to the carbapenems.[3] Increasing numbers of carbapenem-resistant *A. baumannii* isolates have been reported worldwide.[4] The majority of such bacteria are extensively drug resistant, which may include resistance to carbapenems and all other antibiotics except polymyxins and tigecycline.[5] Polymyxin B is effective against drug-resistant *A. baumannii*, but systemic application carries risk of toxicity, primarily kidney toxicity and neurotoxicity.[6,7] *A. baumannii* infection is common in patients with severe infections, and is often accompanied by other bacterial and/or fungal infections.[8] Patients infected with resistant *A. baumannii* have high mortality.[9] Therefore, there is an urgent need to find suitable therapeutic drugs for the treatment of resistant *A. baumannii* infections.

The ineffectiveness of synthetic antibiotics against drug-resistant bacteria has led to the reemergence of interest in silver, which has an ancient history as an antibacterial agent.[10–12] The antibacterial activity of silver nanoparticles (AgNPs) had been reported against multiple species of bacteria; for example, *Escherichia coli* ATCC 8739,[13] *Staphylococcus aureus* ATCC1431,[14] *Escherichia fergusonii*, and *Klebsiella aerogenes* ATCC

Correspondence: Mei Ge
Shanghai Laiyi Center for Biopharmaceutical R&D, No 800, Dongchuan Road, Shanghai 200240, People's Republic of China
Tel/fax +086 21 3420 4838
Email gemei@yeah.net

Xiaodong Cheng
Department of Integrative Biology & Pharmacology, the University of Texas Health Science Center, Houston, USA
Tel/fax +00171 3500 7487
Email xiaodong.cheng@uth.tmc.edu

submit your manuscript | www.dovepress.com
Dovepress
http://dx.doi.org/10.2147/IJN.S104166

1950,[15] among others. Synthesized AgNPs with capping agents, such as citrate, sodium dodecyl sulfate, and polyvinylpyrrolidone show increased antibacterial activity against *S. aureus* and *E. coli*.[16] Huang et al reported antimicrobial activity against *A. baumannii* with the synergistic combination of chitosan acetate and AgNPs.[17] Jain et al studied the interaction of AgNPs with commonly used antibiotics in *Pseudomonas aeruginosa*,[15] while Morones-Ramirez et al demonstrated that Ag^+ treatment sensitized Gram-negative bacteria to the Gram-positive-specific antibiotic vancomycin, both in vitro and in vivo.[18] However, the synergistic antimicrobial activity of antibiotics combined with citrate-capped AgNPs has yet to be studied.

In the present study, we investigated the synergistic combinatorial effects of antibiotics with AgNPs against drug-resistant *A. baumannii* obtained from clinical patients both in vivo and in vitro. We also investigated the possible mechanisms of this synergistic effect.

Materials and methods

Materials

Trisodium citrate, silver nitrate ($AgNO_3$), and sodium borohydride ($NaBH_4$) were used for the synthesis of AgNPs. Rifampicin, tigecyline, polymyxin B (PMB), mucin, dimethyl sulfoxide, 3-(4,5-dimethylthiazol-2-yl)-2,5-diphenyltetrazolium bromide (MTT), isopropyl-β-D-thiogalactoside, penicillin–streptomycin, and trypsin–ethylenediaminetetraacetic acid were purchased from Sigma Aldrich (St Louis, MO, USA). A549 cells and HL-7702 cells were purchased from the Type Culture Collection of the Chinese Academy of Sciences (Shanghai, People's Republic of China). Roswell Park Memorial Institute-1640 medium was purchased from Thermo Fisher Scientific (Waltham, MA, USA) and fetal bovine serum was purchased from HyClone (Logan, UT, USA). No ethical committee approval was required for this set of experiments because the experiments were performed on commercially available cell lines and were considered exempt from full review by the ethics Committee at Shanghai Jiao Tong University.

All animal procedures were approved by the Institutional Animal Care and Use Committee at Shanghai Jiao Tong University. All the animal studies were performed according to the Guiding Principles for the Care and Use of Laboratory Animals according to the Regulations of the People's Republic of China for Administration of Laboratory Animals. All animal procedures were approved by the Animal Ethics Committee of Shanghai Jiao Tong University. C57BL/6 mice were purchased from Slac Laboratory Animal Co., Ltd. (Shanghai, People's Republic of China).

Synthesis and characterization of AgNPs

In a three-necked round-bottomed flask, 20 mL trisodium citrate (1%) and 75 mL ultrapure water were mixed for 15 minutes at 70°C. To the solution, 1.5 mL of silver nitrate solution (1%) was added; $NaBH_4$ (1%) was then added, followed by rapid mixing. This mixed solution was heated for 60 minutes, cooled to room temperature, and water was added to a volume of 100 mL.

To characterize the morphology of the synthesized AgNPs, transmission electron microscopy (TEM) analysis was performed using a Tecnai G2 Spirit 120 kV TEM instrument (0.23 nm resolution) (FEI Company, Hillsboro, OR, USA).

AgNPs were further characterized by scanning the absorbance spectra in 300–500 nm range of wavelength with a multifunction full wavelength microplate analyzer (BioTek Co., Winooski, VT, USA).

A Malvern Zetasizer Nano-ZS instrument (Malvern, Louis, USA) was used to characterize the zeta potential of the nanoparticles in the solution. Data were obtained and analyzed using Zetasizer software (Malvern, Louis, USA).

Determination of minimum inhibitory concentration and fractional inhibitory concentration

The bacterial strain *A. baumannii* (aba 1604; Fudan University Huashan Hospital, Shanghai, People's Republic of China) was used as a model test strain to determine the antibacterial activity of AgNPs. Various concentrations of AgNPs were incubated with 4×10^5 bacteria in Luria Bertani (LB) broth medium in 96-well round-bottomed plates. Bacteria were harvested at the indicated time points and the optical density of the samples was assayed at 600 nm. All samples were plated in triplicate, and values were averaged from three independent trials. The resistant *A. baumannii* strain (aba1604) was made from clinical patients and following institutional ethical guidelines that were reviewed and approved by the ethics committee at the Huashan hospital clinical ethics committee, Fudan University. Consent from clinical patients was not deemed necessary by the Shanghai Laiya centre for Biopharmaceutical R & D who obtained these strains for antibacterial drug research and collected these samples, as the sample collection was part of normal patient care.

To evaluate the antibacterial activity of AgNPs in combination with antibiotics, a two-dimensional microdilution assay was used.[19] Assays were carried out in LB broth growth medium. Minimum inhibitory concentration (MIC) for each of the antibiotics was first estimated, and the fractional inhibitory concentration (FIC) of a combination of antibiotics

and AgNPs was subsequently determined by the checkerboard microtitration method in a 96-well microtiter plate. Antibiotics and AgNPs were diluted to the following concentrations (2MIC, 1MIC, 1/2MIC, 1/4MIC, 1/8MIC, 1/16MIC, and 1/32MIC) in the two-dimensional microdilution assay.

The plates were incubated at 37°C for 18 hours, and results were assayed by measuring the optical density $(OD)_{600}$. The combined antibiotic effect of agents A and B (where A is either $AgNO_3$ or AgNPs, and B is one of three antibiotic agents) was calculated as follows:

$$\text{The FIC index:} = \frac{\text{MIC (A in combination with B)}}{\text{MIC (A alone)}} + \frac{\text{MIC (B in combination with A)}}{\text{MIC (B alone)}} \quad (1)$$

FIC index values above 4.0 indicate antagonistic effects, values between 0.5 and 4.0 indicate additive effects, and values lower than 0.5 indicate synergistic effects.[20]

Cytotoxicity assay

To determine the cytotoxic activity of the AgNPs on mammalian cells, A549 cells and HL-7702 cells (1×10^4 cells/mL) were grown in Roswell Park Memorial Institute-1640 medium containing 5% fetal bovine serum in a 96-well plate at 37°C in an atmosphere of 5% CO_2 for 24 hours. Cells were treated with AgNPs, $AgNO_3$, or control solutions at concentrations ranging from 0.625 to 10 μg/mL for another 24 hours. To determine the viability, MTT (at a concentration of 0.1 mg/mL) was added to the wells and incubated for 4 hours at 37°C and 5% CO_2 to allow cell growth.[21] In metabolically active cells, MTT was reduced to an insoluble, dark purple formazan. The purple formazan was then dissolved in dimethyl sulfoxide. The absorbance was measured at 570 nm using a multifunction full wavelength microplate analyzer and readings were compared from untreated cells. The OD values were used to sort out the percentage of viable cells by using the following formula:

$$\text{Percentage of viability} = \frac{\text{OD value of experimental sample}}{\text{OD value of experimental control (untreated)}} \times 100 \quad (2)$$

Assay for antimicrobial activity in vivo

Minimum lethal dose of $AgNO_3$ or AgNPs in mice

Six-week-old male C57BL/6 mice (body weight ~20 g) were used for all animal experiments. Mice were housed in a temperature- and humidity-controlled environment, and had free access to food and water. Ten mice per group were given intraperitoneal injections of 100 μL total volume. Mice were treated as follows: no treatment, and 10, 20, 40, and 80 mg/kg AgNPs and $AgNO_3$. Injected animals were observed for 3 days.

Determination of minimum lethal dose of *A. baumannii* for peritonitis mouse model

Serial dilutions of *A. baumannii* ranging from 1×10^7 to 1×10^{11} CFU, in 500 μL sterile saline supplemented with 8% mucin, were injected into the peritoneal cavity of mice.[18] Animals were observed for 2 days for determination of the survival rate.

Survival assays

Mice received intraperitoneal injections of the minimum lethal dose (MLD) of *A. baumannii*, with a total volume of 500 μL with 8% mucin. After 1 hour, ten mice in each group received a 100 μL intraperitoneal injection of either vehicle phosphate buffer saline (PBS) or one of the different antibacterial treatments. Mice were observed for 2 days to evaluate the survival rate.

Bacterial colonization assays

Surviving mice were euthanized and dissected, and their kidneys and lungs were collected. These organs were ground under aseptic conditions, and the homogenates were dissolved in sterilized saline water. These organ homogenates were then cultivated on LB plates at 37°C for 24 hours.

Cytokine profiling

Cytokine concentrations in the mouse plasma were measured at the indicated time after infection by standard enzyme-linked immunosorbent assay kits following the manufacturer's instructions (Elabscience Biotechnology Co., Ltd, Wuhan, People's Republic of China).

Antisense RNA models for detecting the synergistic mechanism of AgNPs and antibiotic combinations

To investigate the pathways involved in the bacterial response to AgNPs, we conducted a series of experiments in which the impacts of AgNPs and $AgNO_3$ on different *E. coli* antisense RNA-induced gene-silencing strains were examined.[22–24] The various gene-silenced strains were arrayed in microwell plates, and then screened to determine how their sensitivity to each of the different Ag formulations compared to the parent strain. The gene-silenced *E. coli* strains were treated with isopropyl-β-D-thiogalactoside at appropriate concentrations (Table 1), and portions of the culture were transferred into 96-well plates. Sublethal concentrations of AgNPs, $AgNO_3$, rifampicin,

Table 1 The optimal concentration of IPTG for antisense RNA strains

Genes	Target genes function	IPTG (μmol/L)
ligA	DNA biosynthesis	800
dnaB	Replicative DNA helicase, DNA biosynthesis	20
rpsR	Small subunit ribosomal protein S18, ribosome	10
rpsA	Small subunit ribosomal protein S1, ribosome	40
rpsL	Large subunit ribosomal protein L7/L12, ribosome	10
rplC	Large subunit ribosomal protein L3, ribosome	20
rplT	Large subunit ribosomal protein L20, ribosome	40
rplS	Large subunit ribosomal protein L19, ribosome	40
rpmA	Large subunit ribosomal protein L27, ribosome	60
murA	UDP-*N*-acetylglucosamine 1-carboxyvinyltransferase, peptidoglycan biosynthesis	20
murB	UDP-*N*-acetylenolpyruvoylglucosamine reductase, peptidoglycan biosynthesis	40
murG	Peptidoglycan biosynthesis	40
murE	UDP-*N*-acetylmuramoylalanyl-D-glutamate–2,6-diaminopimelate ligase, peptidoglycan biosynthesis	40
leuS	Leucyl-tRNA synthetase, aminoacyl-tRNA biosynthesis	40
tufA	Elongation factor Tu, protein biosynthesis	40
rpoD	Principal σ factor , RNA biosynthesis	40
fabI	Enoyl-[acyl-carrier protein] reductase I, fatty acid biosynthesis	40
kdsA	Lipopolysaccharides biosynthesis	1,600
kdsB	Lipopolysaccharides biosynthesis	1,600
lpxC	Lipopolysaccharides biosynthesis	1,600
lepB	Signal peptidase, protein export	40
mutL	DNA mismatch repair protein MutL, mismatch repair	40
menD	Ubiquinone and other terpenoid-quinone biosynthesis	40

Abbreviations: IPTG, isopropyl-β-D-thiogalactoside; tRNA, transfer RNA; UDP, uridine diphosphate.

tigecyline, and PMB were added to the gene-silenced bacteria in 96-well plates. Finally, the plates were incubated at 37°C for 16 hours and shaken at 80 rpm. Absorbance was measured at 600 nm using a multifunction full wavelength microplate analyzer, and OD values were used to calculate the inhibition ratio (I) by using the following formula:

$$\text{I}(\%) = \frac{\text{OD value of control (untreated)} - \text{OD value of sample}}{\text{OD value of control (untreated)}} \times 100 \quad (3)$$

$$\Delta\text{I}(\%) = \text{I}_{\text{antisense RNA-induced gene-silencing strains}} - \text{I}_{E.coli\ \text{DH5}\alpha/\text{pHN678}} \quad (4)$$

Statistical analysis

Each assay was repeated three times. Data are presented as mean ± standard deviation, unless otherwise noted. Comparisons between multiple groups were made using one-way analysis of variance (ANOVA) and all analyses were performed using SPSS 21.0 statistical software (21.0; IBM Corporation, Armonk, NY, USA). The threshold for statistical significance was set at $P<0.05$.

Results

Characterization of AgNPs

Based on the image in Figure 1A, AgNPs stabilized by citrate had good dispersion. The particle size distribution was shown by counting AgNPs particle numbers based on TEM images and the histogram of particle size distribution was in Figure 1B. AgNPs were 5–12 nm in diameter, with an average size of 8.4 nm. The nanoparticles were found to be stable for over 6 months, even at 37°C. The zeta potential of the synthesized AgNPs is summarized in Figure 1C. The ultraviolet–visible (UV–vis) spectra of the solution samples are reported in Figure 1D. A single strong peak was observed at 392 nm, which indicates the synthesis of spherical nanoparticles. In practice, dispersion was stable if the zeta potential was higher than 30 mV or less than −30 mV. Supporting the earlier statement, we observed that AgNPs dispersed in water were highly stable with a zeta potential value of −44.5 mV.

Antibacterial activities of AgNP combination treatments

Combination antibiotic therapy is a strategy often employed in the treatment of multiple drug resistance (MDR) *A. baumannii*. Because PMB, rifampicin, and tigecycline are all commonly used against MDR *A. baumannii* in combination with other antibiotics,[25–27] we selected these three antibiotics to evaluate potential combinatorial effects with AgNPs. It was seen that AgNPs displayed potent antimicrobial activity against *A. baumannii*, with an MIC of approximately 2.5 μg/mL, similar to that of $AgNO_3$. Typical drug

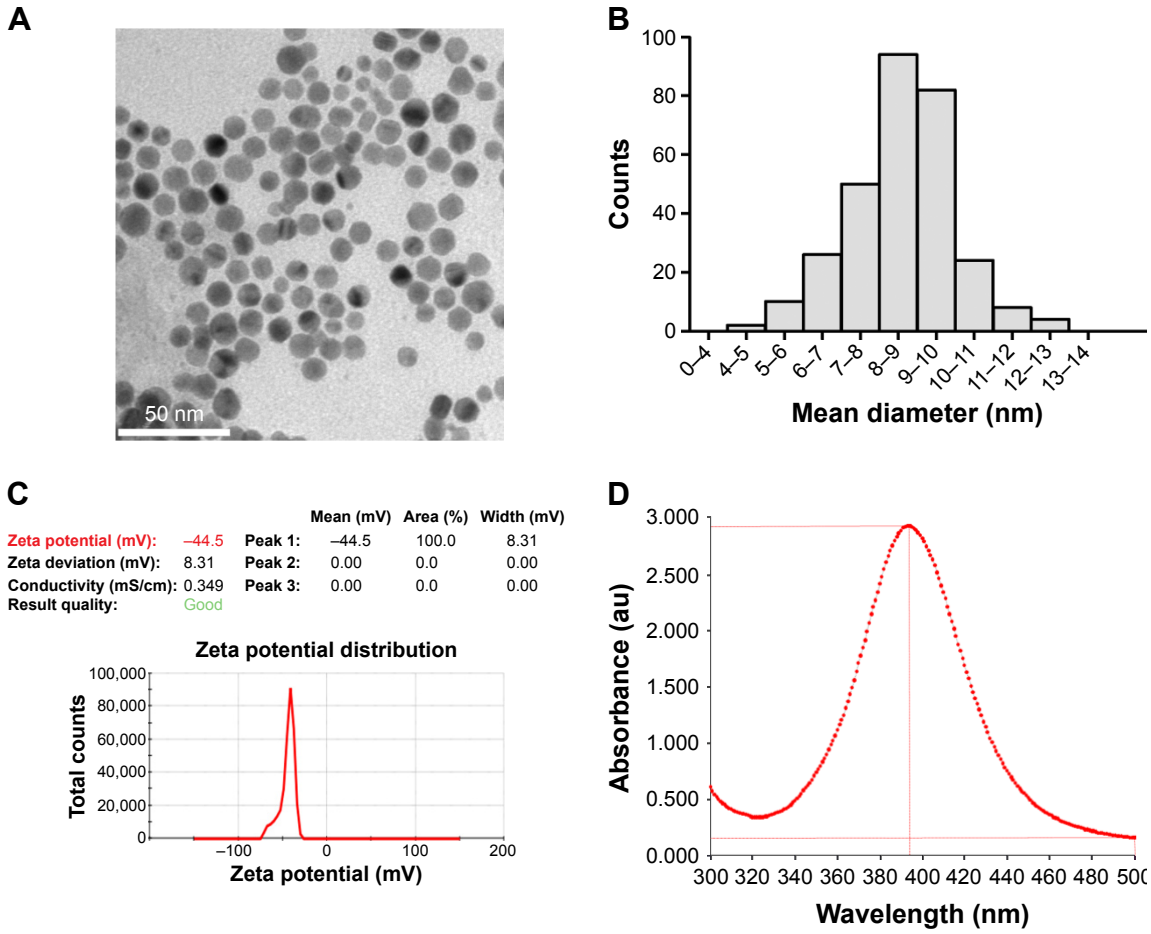

Figure 1 Appearance and physicochemical characteristics of AgNPs.
Notes: (**A**) TEM of AgNPs. (**B**) Size distribution of AgNPs based on TEM images. (**C**) Zeta potential analysis of AgNPs. (**D**) UV–visible absorption spectroscopy showed the maximum absorbance at 392 nm for AgNPs.
Abbreviations: AgNPs, silver nanoparticles; OD, optical density; TEM, transmission electron microscopy; UV, ultraviolet.

MICs, summarized in Table 2, were 0.25 μg/mL for PMB, 3.12 μg/mL for rifampicin, and 3.12 μg/mL for tigecycline.

The FIC of AgNPs and the various antibiotic combinations were investigated and are summarized in Table 2. These experiments showed that PMB and rifampicin acted synergistically ($P<0.5$) with AgNPs and $AgNO_3$, while tigecycline did not show synergy ($P>0.5$) with either AgNPs or $AgNO_3$.

Table 2 FIC index of combinations among silver and antibiotics against *Acinetobacter baumannii*

Compounds	FIC of AgNPs	FIC of $AgNO_3$	MIC of antibiotics (μg/mL)
Polymyxin B	0.19	0.19	0.25
Rifampicin	0.38	0.38	3.12
Tigecycline	0.75	0.75	3.12
AgNPs	–	–	2.5
$AgNO_3$	–	–	2.5

Note: Data are presented as mean ± SD, unless otherwise specified.
Abbreviations: FIC, fractional inhibitory concentration; MIC, minimum inhibitory concentration; AgNPs, silver nanoparticles; SD, standard deviation.

Cytotoxicity of AgNPs in vitro

Many investigations have reported on the inhibitory effects of AgNPs on cells. For example, Beer et al found that AgNPs inhibited the proliferation of A549 cells in a dose-dependent manner,[28] whereas Foldbjerg et al reported that AgNPs induced increase in reactive oxygen species (ROS) level in A549 cells.[29] Here, we used the method described by Foldbjerg et al to evaluate the cytotoxicity of AgNPs.[29]

As shown in Figure 2, high concentrations of $AgNO_3$ significantly affected cell growth. By comparison, exposure to AgNPs at a higher concentration of 10 μg/mL did not exhibit significant cytotoxicity in A549 and HL-7702 cells. These results demonstrate that the cytotoxicity of AgNPs is lower than that of $AgNO_3$.

Effects of AgNPs on antimicrobial activity in vivo

The acute toxicity of AgNPs and $AgNO_3$ were measured in vivo to establish the median lethal dose (LD_{50}) (Figure 3).

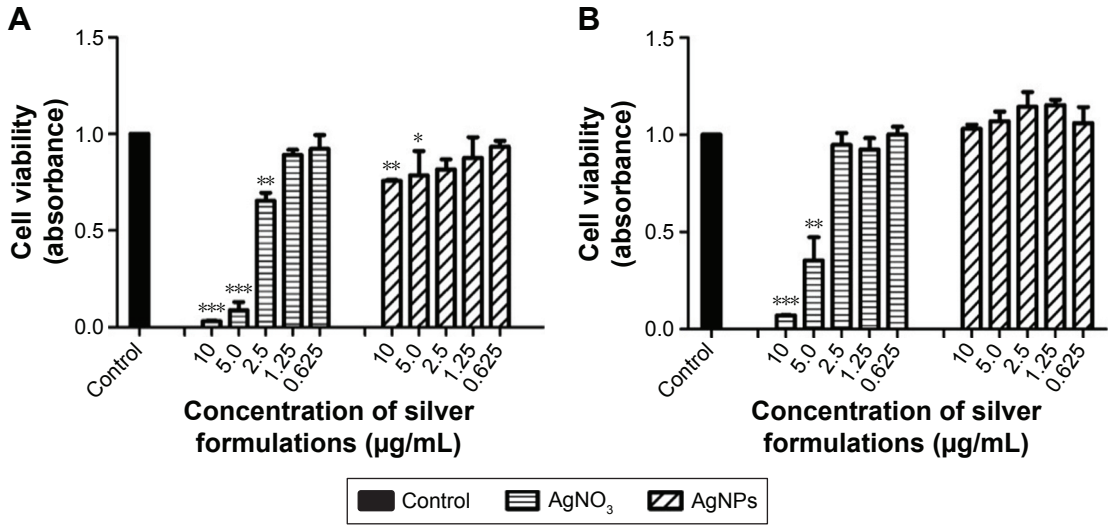

Figure 2 Relative survival of A549 and HL-7720 cells exposed to AgNPs.
Notes: Relative survival of cells as affected by different doses AgNPs or $AgNO_3$. (**A**) MTT assay results confirmed the in vitro cytotoxicity of AgNPs and $AgNO_3$ against A549 cells. (**B**) Effects of AgNPs or $AgNO_3$ on HL-7720 cell growth. Results are shown as the mean ± SD of three independent experiments. *$P<0.05$, **$P<0.01$ and ***$P<0.001$ vs control.
Abbreviations: AgNPs, silver nanoparticles; MTT, 3-(4,5-dimethylthiazol-2-yl)-2,5-diphenyltetrazolium bromide; SD, standard deviation.

The LD_{50} of AgNPs was determined to be between 20 and 40 mg/kg, and the LD_{50} of $AgNO_3$ was also found to be between 20 and 40 mg/kg. These LD_{50} values for $AgNO_3$ are similar to those reported in an earlier toxicity study.[18]

Infection was established in mice through intraperitoneal delivery of 5×10^9 *A. baumannii* cells suspended in an aqueous solution containing 8% mucin. Within 24 hours after the time of injection, all infected mice had died. Thus, *A. baumannii* was used at this same concentration of 5×10^9 cells for all subsequent experiments.

The PMB and AgNPs combination and the PMB and $AgNO_3$ combination showed the same synergistic antibiotic effects that we had earlier observed in vivo (Figure 4). We observed the mice living condition for 1 week, and calculated 2 days survival rate. A mixture of $AgNO_3$ and PMB (3 mg/kg and 10 μg/kg, respectively) resulted in a survival rate of 40%. When either of these two compounds was given alone as a single-dose treatment, survival rates were 0%. By comparison, even a low-dosage mixture of AgNPs and PMB (2 mg/kg and 10 μg/kg, respectively) resulted in a high survival rate of 60%.

Two days after administration in mice, we dissected a portion of mice for bacterial colonization assay. Representative images of bacterial growth are presented in Figure 5, which show that $AgNO_3$ and AgNPs enhanced the action of

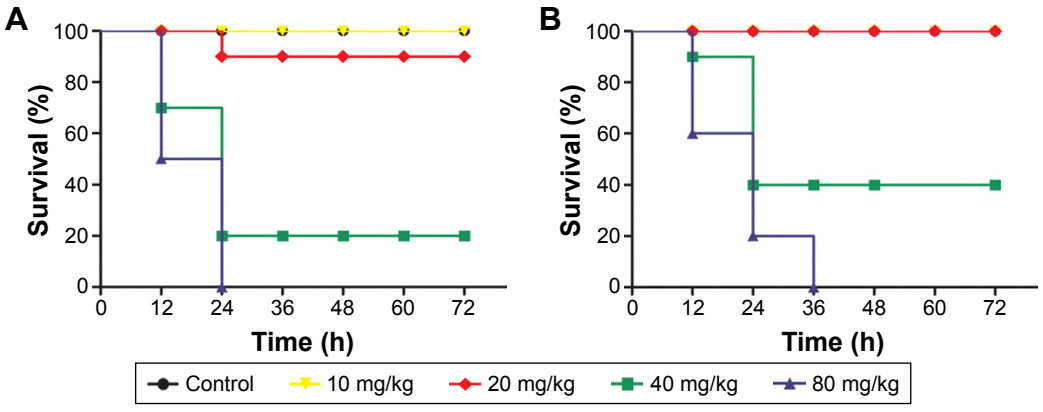

Figure 3 Toxicity of AgNPs and $AgNO_3$ in mice.
Notes: (**A**) Survival of mice given the following treatments: control, 10, 20, 40, and 80 mg/kg $AgNO_3$. (**B**) Survival of mice given the following treatments: control, 10, 20, 40, or 80 mg/kg AgNPs. Survival assays were performed with ten mice per group.
Abbreviations: AgNPs, silver nanoparticles; h, hours.

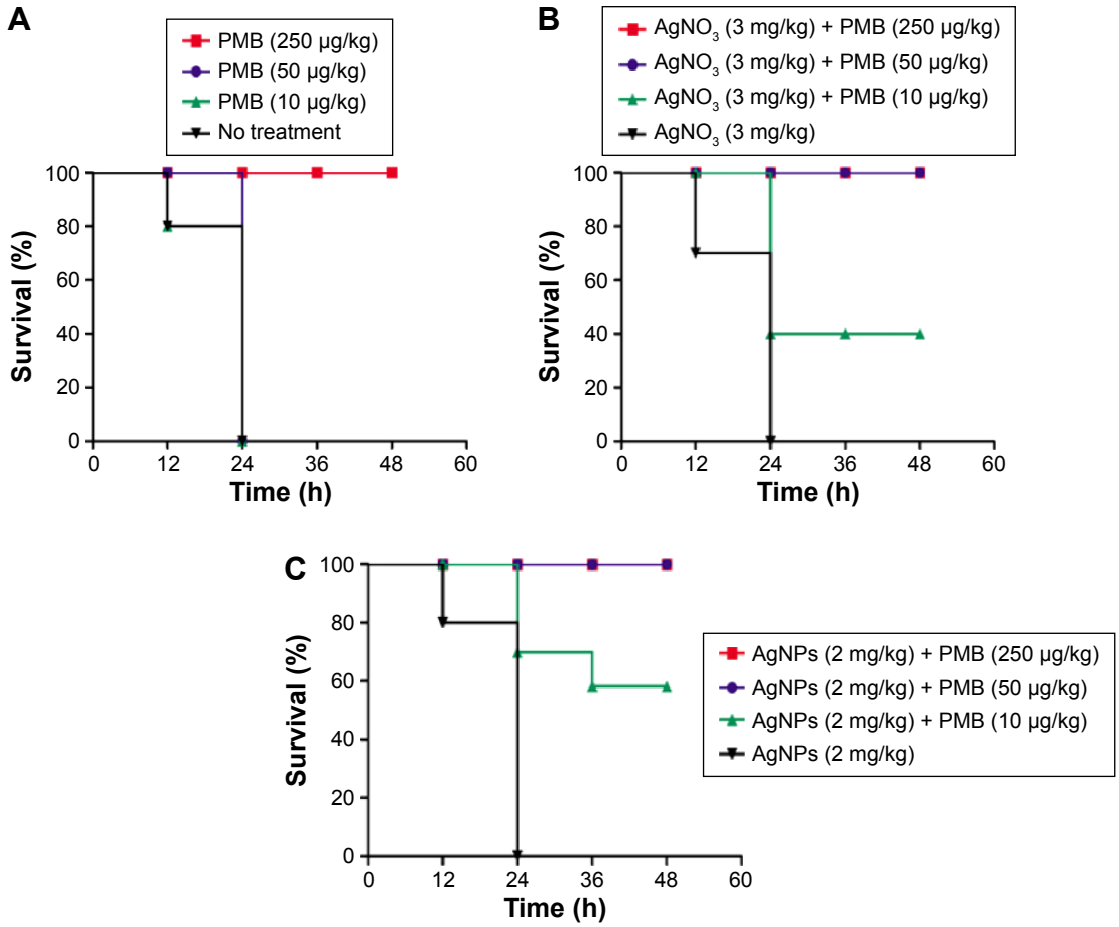

Figure 4 Survival of mice given AgNPs or $AgNO_3$ with PMB in a peritonitis infection model.
Notes: (**A**) PMB treatment concentration in peritonitis infection model. (**B**) $AgNO_3$ and PMB treatment concentration in peritonitis infection model. (**C**) AgNPs and PMB treatment concentration peritonitis infection model.
Abbreviations: AgNPs, silver nanoparticles; PMB, polymyxin B; h, hours.

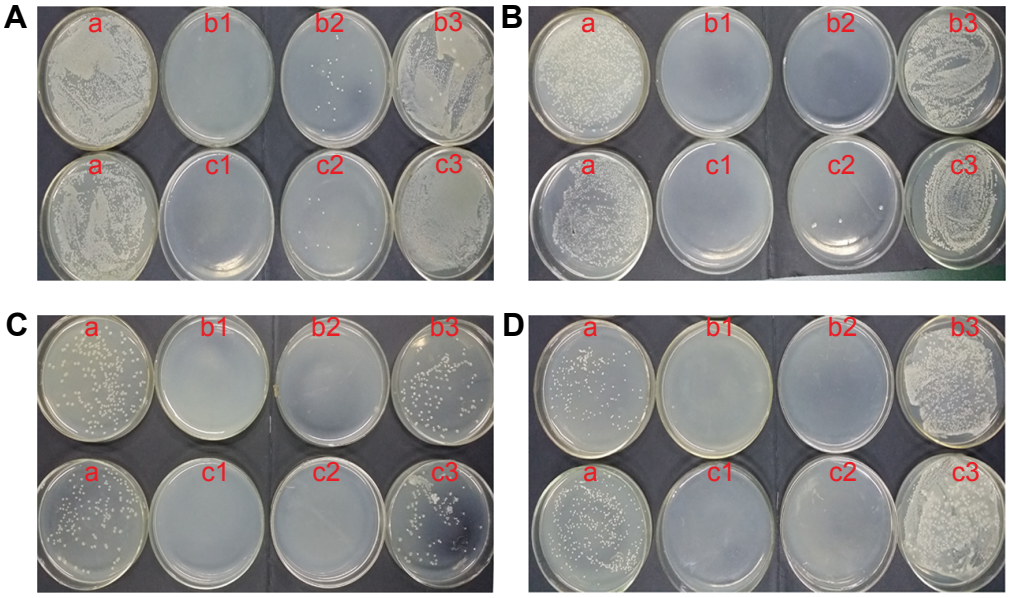

Figure 5 Bacterial burdens in *Acinetobacter baumannii*-infected mice after treatment with PMB combined with $AgNO_3$ or AgNPs.
Notes: Bacterial burdens in *Acinetobacter baumannii*-infected mice after treatment with PMB (250 μg/kg) (a); the infected mice after treatment with PMB combined with $AgNO_3$ (3 mg/kg, 18 μM) (b1: 250 μg/kg; b2: 50 μg/kg; b3: 10 μg/kg), and with AgNPs (2 mg/kg, 18 μM) (c1–c3). (**A**) kidney; (**B**) lung; (**C**) blood; (**D**) ascitic fluid.
Abbreviations: AgNPs, silver nanoparticles; PMB, polymyxin B.

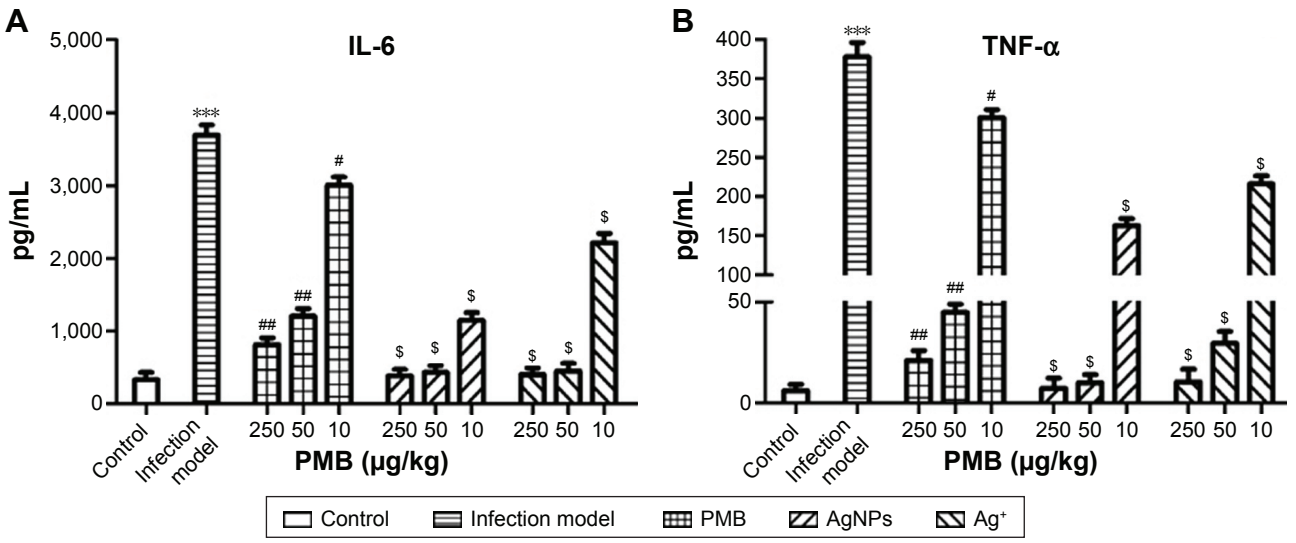

Figure 6 $AgNO_3$ or AgNPs combined with antibiotics-modulated *Acinetobacter baumannii*-induced inflammatory reaction.
Notes: ELISA was used to measure IL-6 (**A**) and TNF-α (**B**) in the mouse plasma 18 hours post infection. Results are shown as the mean ± SD of three independent experiments. ***$P<0.001$ vs control; #$P<0.05$ and ##$P<0.01$ vs infection model; $P<0.05$ vs PMB only group. We obtained *P*-values by a Students' *t*-test.
Abbreviations: ELISA, enzyme-linked immunosorbent assay; IL, interleukin; PMB, polymyxin B; TNF-α, tumor necrosis factor alpha; SD, standard deviation.

PMB against *A. baumannii* in peritonitis infection model. Figure 5A and B shows that there are plenty of bacteria present in both the kidney and lungs when animals are treated with PMB alone at a dose of 250 μg/kg. With the addition of $AgNO_3$ (3 mg/kg, 18 μM) or AgNPs (2 mg/kg, 18 μM), no bacteria were detected in the kidneys or lungs. When we reduced the PMB dose to 50 μg/kg, we found that the kidney and lung tissues contained only a small amount of bacteria. Further reduction of the PMB dose to 10 μg/kg was less effective, leaving a substantial bacterial burden in the kidney and lungs. Moreover, we also tested the blood and ascites of infected mice and found that they did not contain bacteria under the combined administration of PMB (50 μg/kg) with either $AgNO_3$ (3 mg/kg, 18 μM) or AgNPs (2 mg/kg, 18 μM) (Figure 5C and D). These results indicate not only that $AgNO_3$ can enhance the antibacterial activity of antibiotics but also that AgNPs possess antibacterial capability in vivo.

To analyze whether $AgNO_3$ or AgNPs combined with antibiotics regulate inflammation during *A. baumannii* infection, we assessed proinflammatory cytokines in the mouse plasma using enzyme-linked immunosorbent assay. The levels of tumor necrosis factor alpha (TNF-α) and interleukin (IL)-6 decreased significantly in the mouse plasma of treated mice compared to those of model mice at 18 hours post infection (Figure 6). $AgNO_3$ and AgNPs could enhance the action of PMB against *A. baumannii* in vivo.

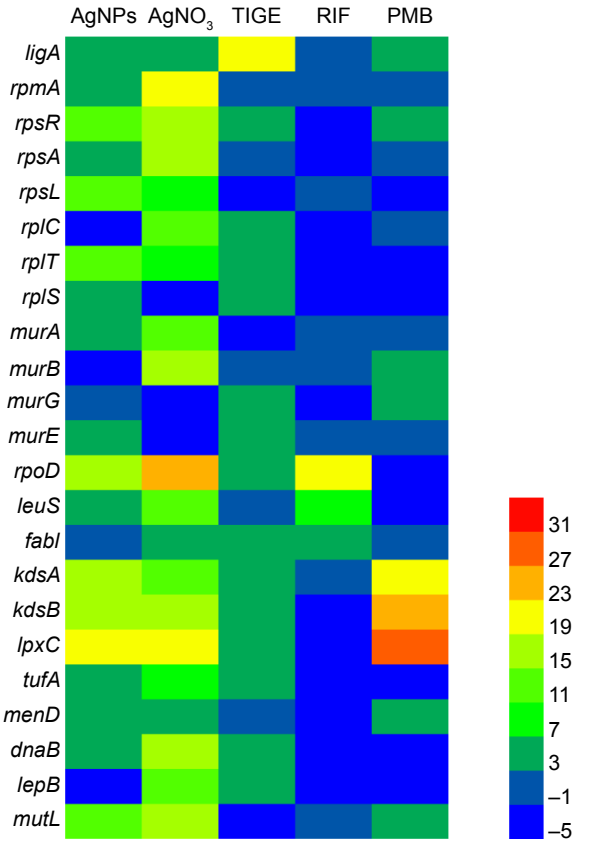

Figure 7 Heat map analysis of sensitivity to AgNPs and $AgNO_3$ in gene-silenced *Escherichia coli* strains relative to the control *E. coli* DH5α/pHN678 strain.
Notes: Each unit represents the difference in inhibition rate between a single antisense RNA-induced gene silencing and the control *E. coli* DH5α/pHN678 strain. Red units represent the most sensitive strains for compounds, and blue represents strains that grow similarly to the control *E. coli* DH5α/pHN678 strain.
Abbreviations: AgNPs, silver nanoparticles; TIGE, tigecycline; RIF, rifampicin; PMB, polymyxin B.

Mechanisms for enhanced antimicrobial activity of AgNPs in combination with antibiotics

To better understand the mechanisms supporting the synergistic effects of AgNPs combined with antibiotics, we used antisense RNA-induced gene silencing to silence the expression of a number of genes in *E. coli* (Figure 7). The difference in inhibition rate between a set of gene-silenced *E. coli* strains and the control *E. coli* DH5α/pHN678 strain is represented by color in our heat map analysis; dark red represents the most sensitive strains, whereas dark blue represents the least sensitive strains, relative to the parent strain. We found that silencing of *rpoD, kdsA, kdsB, lpxC*, and *mutL* resulted in sensitivity to both $AgNO_3$ and AgNPs. Silencing of *rpsR, rpsL, rpsA, murB, murA, leuS*, and *dnaB* led only to sensitivity to $AgNO_3$, which indicates that AgNPs act at a higher selectivity than $AgNO_3$. In addition, the *rpoD*-silenced strain was sensitive to rifampicin, while the silencing of *kdsA, kdsB*, and *lpxC* increased sensitivity to PMB.

Discussion

A. baumannii has been proved to be resistant to many kinds of antibiotics, which is suitable for genetic exchange. Fournier et al reported an 86 kb genomic region naming AbaR1 resistance island in AYE which had 45 resistance genes in the MDR isolate.[30] The key resistance genes were those coding for AmpC, VEB-1, and OXA-10 beta-lactamases, tetracycline efflux pumps, and various aminoglycoside-modifying enzymes. Moreover, Fournier et al found that 17 out of the 22 clinical *A. baumannii* isolates showed an original ATPase ORF. These 17 isolates contained eleven isolates that are resistant to several antibiotic families, including β-lactams, and six other isolates susceptible to β-lactams. AgNPs could damage the membrane potential, prevent ATP production, increase the level of ROS, and damage the membrane lipids as well as DNA, which demonstrated that AgNPs have broad-range antibacterial properties, including *A. baumannii*.[31]

It has been reported that citrate-capped AgNPs are less toxic to mammalian cells and show increased antimicrobial activity against *S. aureus* and *P. aeruginosa*.[32] Our results support these findings, and further build from them to explore the toxicity of AgNPs to A549 and HL-7702 cells, and to describe the effects of AgNPs on drug-resistant *A. baumannii*. Our study demonstrates that the cytotoxicity of AgNPs is lower than that of $AgNO_3$.

The combination of AgNPs and either PMB or rifampicin showed strong synergistic antimicrobial effects. Moreover, the pairing of AgNPs and PMB showed an enhanced effect against *A. baumannii* in vivo, which suggests the possibility of a clinical application for this combination therapy.[33]

IL-6 and TNF-α are cytokines that have been shown to play an important role in the host immune response against intracellular pathogens in murine models. Smani et al demonstrated that *A. baumannii* induced the release of TNF-α and IL-6 and increased the Ca^{2+} influx.[34] The levels of TNF-α and IL-6 decreased significantly in the mouse plasma of treated mice compared to those of model mice, which further proved that inhibiting proinflammatory signals could be protective during *A. baumannii* infections. Sarkar et al reported that AgNPs could modulate human macrophage responses to *Mycobacterium tuberculosis*.[35] *A. baumannii* is also highly correlated with the host immune status.[35] We have verified the role of AgNPs on *A. baumannii*. Hence, we hypothesized that AgNPs could modulate human macrophage responses to *A. baumannii*, as the mode of *M. tuberculosis*.

E. coli is one of the most representative model organisms in experimental biology and medical study; there are a large number of experimental studies on the drug mechanisms and targets using *E. coli*.[22–24] On the one hand, *A. baumannii* is a common clinical pathogen, which has received increased attention.[36] *A. baumannii* and *E. coli* are Gram-negative bacteria, and they have similar cell structure.[37] So we probe the mechanism of synergistic effect of AgNPs and antibiotics combination against *A. baumannii* using *E. coli* as a model system.

The probable role of PMB in such drug synergy is its rapid permeabilization of the outer cell membrane, allowing enhanced penetration by AgNPs. Polymyxin B can displace Mg^{2+} or Ca^{2+}, and also binds to the Lipid A component of lipopolysaccharide (LPS), resulting in changes to the outer membranes of bacteria. Our gene-silencing experiments also suggested that LpxC plays a role in sensitivity toward AgNPs and $AgNO_3$. Lin et al found that an LpxC inhibitor blocked the ability of bacteria to activate the sepsis cascade, enhanced opsonophagocytic killing of *A. baumannii*, and protected mice from lethal infection.[38] Moreover, the potential contributions of PMB and AgNPs both involve Lipid A of LPS, a convergence which supports their synergistic effects.

KDO 2-keto-3-deoxyoctanoic acid (KDO) plays an essential role in LPS biosynthesis, and may serve a universal role in group 2 capsule biosynthesis by linking the polysaccharide region to the lipid domain.[39] The *kdsA* gene encodes the protein KDO 8-phosphate synthetase, which catalyzes

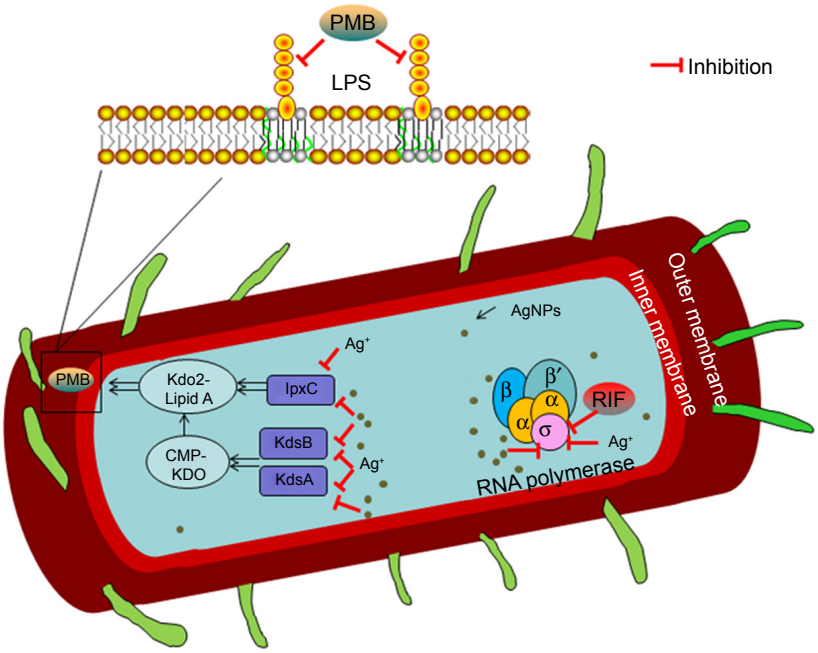

Figure 8 Proposed mechanisms of the combination of AgNPs/Ag^+ with antibiotics against G^+ negative bacterium.
Notes: AgNPs/Ag^+ can enhance PMB-induced damage of the membrane lipids. AgNPs/Ag^+ and RIF also may bind intracellular proteins and RNA polymerase, upon entering the cytosol.
Abbreviations: AgNPs, silver nanoparticles; PMB, polymyxin B; RIF, rifampicin; LPS, lipopolysaccharide; CMP-KDO, cytosine monophosphate-2-keto-3-deoxyoctanoic acid.

the first step of the KDO synthetic reaction.[40] The *kdsB* gene encodes CMP-KDO synthetase, which is essential to the LPS biosynthesis pathway.[41] Our gene-silencing results suggested that *kdsA* and *kdsB* are involved in bacterial sensitivity toward AgNPs and $AgNO_3$, as well as PMB.

Similarly, we observed that silencing of RpoD, which is involved in promoter localization and plays a crucial role in transcription initiation,[42] increased the sensitivity of *E. coli* toward AgNPs and $AgNO_3$. Most of the factors investigated belong to the σ70 family, and all bacteria express one or more σ70 factors. The σ70 factor sequence is highly conserved and plays an important role in bacterial growth. Rifampicin has a molecular mechanism of action that involves inhibition of DNA-dependent RNA polymerase.[43] In *E. coli*, this enzyme is a complex oligomer comprising four subunits: α, β, β′, and σ, encoded, respectively, by *rpoA*, *rpoB*, *rpoC*, and *rpoD*, and their disruption interferes in the transcription process.[43] The potential mechanisms of both rifampicin and AgNPs involve effects on DNA-dependent RNA polymerase, which is the evidence that supports their synergistic effects (Figure 8).

Silver and silver-containing compounds have recently drawn increasing interest as antimicrobial agents for treating bacterial infections. AgNPs showed synergy of inhibiting *P. aeruginosa* biofilms when combined with sub-MIC levels of aztreonam.[44] Combination of AgNPs with ceftazidime also showed a synergy to inhibit *P. aeruginosa*.[45] AgNPs prepared as described by Tiwari et al exhibited tremendous antibacterial activity against a carbapenem-resistant strain of *A. baumannii*.[3] This required an efficient treatment regimen, and the combination of rifampin with imipenem had been evaluated in clinical infections caused by a highly imipenem-resistant *A. baumannii* strain.[46] Yoon et al showed that the combination of PMB plus imipenem was as effective as PMB plus rifampin against a carbapenem-resistant strain of *A. baumannii*.[26] Therefore, drug treatment with newer antimicrobials or antimicrobial combinations has become increasingly important to eradicate these infections. According to our study, the combination of AgNPs with antibiotics could be an effective solution to the problem of carbapenem-resistant strains of *A. baumannii*, potentially at lower and less-toxic doses than what is now typically used clinically.

Investigators have previously suggested that combination drug therapy could be an effective tool to prevent the emergence of bacterial resistance, especially for patients infected with Gram-negative bacteria that have developed resistance to a single therapy.[47] Our study showed the synergistic effects of combining AgNPs and PMB or AgNPs and rifampicin against drug-resistant *A. baumannii* isolated from clinical patients. Considering the lower toxicity of

AgNPs compared to other treatment options, these drug combinations have potential as useful tools for the clinic.

Acknowledgments

The authors are very grateful to Professor Zhu Demei from Fudan University Huashan Hospital, who provided the resistant *A. baumannii* strain (aba1604) from clinical patients.

This work was funded by The National Major Scientific and Technological Special Project for "Significant New Drugs Development" (2012ZX09301002-003-007).

Disclosure

The authors report no conflicts of interest in this work.

References

1. Munoz-Price LS, Weinstein RA. Acinetobacter infection. *New Engl J Med*. 2008;358(12):1271–1281.
2. Peleg AY, Seifert H, Paterson DL. *Acinetobacter baumannii*: emergence of a successful pathogen. *Clin Microbiol Rev*. 2008;21(3):538–582.
3. Tiwari V, Tiwari M. Quantitative proteomics to study carbapenem resistance in *Acinetobacter baumannii*. *Front Microbiol*. 2014;5:512.
4. Poirel L, Nordmann P. Carbapenem resistance in *Acinetobacter baumannii*: mechanisms and epidemiology. *Clin Microbiol Infec*. 2006;12(9):826–836.
5. Dizbay M, Tunccan OG, Sezer BE, Hizel K. Nosocomial imipenem-resistant *Acinetobacter baumannii* infections: epidemiology and risk factors. *Scand J Infect Dis*. 2010;42(10):741–746.
6. Brown JM, Dorman DC, Roy LP. Acute renal failure due to overdosage of colistin. *Med J Australia*. 1970;2(20):923–924.
7. Koch-Weser J, Sidel VW, Federman EB, Kanarek P, Finer DC, Eaton AE. Adverse effects of sodium colistimethate. Manifestations and specific reaction rates during 317 courses of therapy. *Ann Intern Med*. 1970;72(6):857–868.
8. Rodriguez Guardado A, Blanco A, Asensi V, et al. Multidrug-resistant *Acinetobacter meningitis* in neurosurgical patients with intraventricular catheters: assessment of different treatments. *J Antimicrob Chemoth*. 2008;61(4):908–913.
9. Dijkshoorn L, Nemec A, Seifert H. An increasing threat in hospitals: multidrug-resistant *Acinetobacter baumannii*. *Nat Rev Microbiol*. 2007;5(12):939–951.
10. Caruso DM, Foster KN, Hermans MH, Rick C. Aquacel Ag in the management of partial-thickness burns: results of a clinical trial. *J Burn Care Rehabil*. 2004;25(1):89–97.
11. Chen S, Wu G, Zeng H. Preparation of high antimicrobial activity thiourea chitosan–Ag+ complex. *Carbohyd Polym*. 2005;60(1):33–38.
12. Cao XL, Cheng C, Ma YL, Zhao CS. Preparation of silver nanoparticles with antimicrobial activities and the researches of their biocompatibilities. *J Mater Sci Mater Med*. 2010;21(10):2861–2868.
13. Li WR, Xie XB, Shi QS, Zeng HY, Ou-Yang YS, Chen YB. Antibacterial activity and mechanism of silver nanoparticles on *Escherichia coli*. *Appl Microbiol Biotechnol*. 2010;85(4):1115–1122.
14. Mirzajani F, Ghassempour A, Aliahmadi A, Esmaeili MA. Antibacterial effect of silver nanoparticles on *Staphylococcus aureus*. *Res Microbiol*. 2011;162(5):542–549.
15. Kora AJ, Rastogi L. Enhancement of antibacterial activity of capped silver nanoparticles in combination with antibiotics, on model gram-negative and gram-positive bacteria. *Bioinorg Chem Appl*. 2013(8):319–355.
16. Huang L, Dai T, Xuan Y, Tegos GP, Hamblin MR. Synergistic combination of chitosan acetate with nanoparticle silver as a topical antimicrobial: efficacy against bacterial burn infections. *Antimicrob Agents Chemother*. 2011;55(7):3432–3438.
17. Jain J, Arora S, Rajwade JM, Omray P, Khandelwal S, Paknikar KM. Silver nanoparticles in therapeutics: development of an antimicrobial gel formulation for topical use. *Mol Pharm*. 2009;6(5):1388–1401.
18. Morones-Ramirez JR, Winkler JA, Spina CS, Collins JJ. Silver enhances antibiotic activity against gram-negative bacteria. *Sci Transl Med*. 2013;5(190):190ra181.
19. Sopirala MM, Mangino JE, Gebreyes WA, et al. Synergy testing by Etest, microdilution checkerboard, and time-kill methods for pan-drug-resistant *Acinetobacter baumannii*. *Antimicrob Agents Chemother*. 2010;54(11):4678–4683.
20. Odds FC. Synergy, antagonism, and what the chequerboard puts between them. *J Antimicrob Chemoth*. 2003;52(1):1–1.
21. Meng ZX, Nie J, Ling JJ, et al. Activation of liver X receptors inhibits pancreatic islet beta cell proliferation through cell cycle arrest. *Diabetologia*. 2009;52(1):125–135.
22. Goh S, Boberek JM, Nakashima N, Stach J, Good L. Concurrent growth rate and transcript analyses reveal essential gene stringency in *Escherichia coli*. *PloS one*. 2009;4(6):e6061.
23. Singh SB, Phillips JW, Wang J. Highly sensitive target-based whole-cell antibacterial discovery strategy by antisense RNA silencing. *Curr Opin Drug Discov Devel*. 2007;10(2):160–166.
24. Nakashima N, Goh S, Good L, Tamura T. Multiple-gene silencing using antisense RNAs in Escherichia coli. *Methods Mol Biol*. 2012;815:307–319.
25. Timurkaynak F, Can F, Azap OK, Demirbilek M, Arslan H, Karaman SO. In vitro activities of non-traditional antimicrobials alone or in combination against multidrug-resistant strains of *Pseudomonas aeruginosa* and *Acinetobacter baumannii* isolated from intensive care units. *Int J Antimicrob Agents*. 2006;27(3):224–228.
26. Yoon J, Urban C, Terzian C, Mariano N, Rahal JJ. *In vitro* double and triple synergistic activities of Polymyxin B, imipenem, and rifampin against multidrug-resistant *Acinetobacter baumannii*. *Antimicrob Agents Chemother*. 2004;48(3):753–757.
27. Scheetz MH, Qi C, Warren JR, et al. *In vitro* activities of various antimicrobials alone and in combination with tigecycline against carbapenem-intermediate or -resistant *Acinetobacter baumannii*. *Antimicrob Agents Chemother*. 2007;51(5):1621–1626.
28. Beer C, Foldbjerg R, Hayashi Y, et al. Toxicity of silver nanoparticles – nanoparticle or silver ion?. *Toxicol Lett*. 2012;208(3):286–292.
29. Foldbjerg R, Dang DA, Autrup H. Cytotoxicity and genotoxicity of silver nanoparticles in the human lung cancer cell line, A549. *Arch Toxicol*. 2011;85(7):743–750.
30. Fournier PE, Vallenet D, Barbe V, et al. Comparative genomics of multidrug resistance in *Acinetobacter baumannii*. *PLoS Genet*. 2006;2(1):e7.
31. Rizzello L, Pompa PP. Nanosilver-based antibacterial drugs and devices: mechanisms, methodological drawbacks, and guidelines. *Chem Soc Rev*. 2014;43(5):1501–1518.
32. Flores CY, Minan AG, Grillo CA, Salvarezza RC, Vericat C, Schilardi PL. Citrate-capped silver nanoparticles showing good bactericidal effect against both planktonic and sessile bacteria and a low cytotoxicity to osteoblastic cells. *ACS Appl Mater Interfaces*. 2013;5(8):3149–3159.
33. Lambadi PR, Sharma TK, Kumar P, et al. Facile biofunctionalization of silver nanoparticles for enhanced antibacterial properties, endotoxin removal, and biofilm control. *Int J Nanomed*. 2015;10:2155–2171.
34. Smani Y, Docobo-Pérez F, Mcconnell MJ, et al. *Acinetobacter baumannii*-induced lung cell death: role of inflammation, oxidative stress and cytosolic calcium. *Microb Pathogenesis*. 2011;50(5):224–232.

35. Sarkar S, Leo BF, Carranza C, et al. Modulation of human macrophage responses to *Mycobacterium tuberculosis* by silver nanoparticles of different size and surface modification. *PLoS One*. 2015;10(11).
36. Perez F, Hujer AM, Hujer KM, et al. Global challenge of multidrug-resistant *Acinetobacter baumannii*. *Antimicrob Agents Ch*. 2007;51(10):3471–3484.
37. Gootz TD. The forgotten Gram-negative bacilli: what genetic determinants are telling us about the spread of antibiotic resistance. *Biochem Pharmacol*. 2006;71(7):1073–1084.
38. Lin L, Tan B, Pantapalangkoor P, et al. Inhibition of LpxC protects mice from resistant *Acinetobacter baumannii* by modulating inflammation and enhancing phagocytosis. *MBio*. 2012;3(5):429–493.
39. Raetz CR, Whitfield C. Lipopolysaccharide endotoxins. *Annu Rev Biochem*. 2002;71:635–700.
40. Ray PH. Purification and characterization of 3-deoxy-D-manno-octulosonate 8-phosphate synthetase from *Escherichia coli*. *J Bacteriol*. 1980;141(2):635–644.
41. Meredith TC, Woodard RW. Characterization of *Escherichia coli* D-arabinose 5-phosphate isomerase encoded by kpsF: implications for group 2 capsule biosynthesis. *Biochem J*. 2006;395(2):427–432.
42. Donohue TJ. Targeted sigma factor turnover inserts negative control into a positive feedback loop. *Mol Microbiol*. 2009;73(5):747–750.
43. McClure WR, Cech CL. On the mechanism of rifampicin inhibition of RNA synthesis. *J Biol Chem*. 1978;253(24):8949–8956.
44. Habash MB, Park AJ, Vis EC, et al. Synergy of silver nanoparticles and aztreonam against *Pseudomonas aeruginosa* PAO1 biofilms. *Antimicrob Agents Ch*. 2014;58(10):5818–5830.
45. Jain J, Arora S, Rajwade JM, et al. Silver nanoparticles in therapeutics: development of an antimicrobial gel formulation for topical use. *Mol Pharm*. 2009;6(5):1388–1401.
46. Saballs M, Pujol M, Tubau F, et al. Rifampicin/imipenem combination in the treatment of carbapenem-resistant *Acinetobacter baumannii* infections. *J Antimicrob Chemoth*. 2006;58(3):697–700.
47. Mouton JW. Combination therapy as a tool to prevent emergence of bacterial resistance. *Infection*. 1999;27(Suppl 2):S24–S28.